Probehead with interchangeable tunable bridged loop-gap resonator for pulsed zero-field optically detected magnetic resonance experiments on photoexcited triplet states

V. Weis, W. Mittelbach, J. Claus, K. Möbius, and T. Prisner

Articles you may be interested in

Pulsed electron nuclear double resonance studies of the photoexcited triplet state of pentacene in p -terphenyl crystals at room temperature
J. Chem. Phys. **127**, 114503 (2007); 10.1063/1.2771145

Zero-field electron spin resonance and theoretical studies of light penetration into single crystal and polycrystalline material doped with molecules photoexcitable to the triplet state via intersystem crossing
J. Chem. Phys. **117**, 4940 (2002); 10.1063/1.1499124

Quasi-static numerical analysis of loop-gap resonator
AIP Conf. Proc. **557**, 454 (2001); 10.1063/1.1373792

Zero-field magnetic resonance of the photo-excited triplet state of pentacene at room temperature
J. Chem. Phys. **113**, 11194 (2000); 10.1063/1.1326069

A pulsed ENDOR probehead with the bridged loopgap resonator: Construction and performance
Rev. Sci. Instrum. **61**, 3360 (1990); 10.1063/1.1141584

Probehead with interchangeable tunable bridged loop-gap resonator for pulsed zero-field optically detected magnetic resonance experiments on photoexcited triplet states

V. Weis, W. Mittelbach, J. Claus, K. Möbius, and T. Prisner

Institut für Experimentalphysik, Arnimallee 14, 14 195 Berlin, Germany

Conventional zero-field optically detected magnetic resonance (ODMR) is normally performed by using a slow-wave helix for microwave excitation with a quality factor Q≈1. With available microwave sources this low Q factor leads to long microwave pulse lengths for coherent pulse experiments (π-pulse duration of about 300 ns for 20 W microwave excitation power). For our zero-field experiments we took advantage of the bridged loop-gap microwave resonator configuration with relatively high Q factor. Without the possibility of tuning the Zeeman energy level splitting as in electron paramagnetic resonance (EPR), in zero-field ODMR the resonator has to cover a wide range of frequencies. We are able to tune our probehead in the range of 1.9–8 GHz with a loaded Q factor of up to 800 by using interchangeable bridged loop-gap resonators of various designs. Thereby, the pulse lengths, compared to the slow-wave helix, could be reduced by nearly one order of magnitude ($t_{\mathrm{resonator}}^{\pi}=45$ ns employing the same microwave power of 20 W). Experimental data are presented for triplet states of photoexcited acridine and benzophenone molecules at different resonance frequencies for their $|T_x\rangle - |T_z\rangle$ transitions ($\nu=2.472$ GHz and $\nu=5.226$ GHz), respectively. © *1997 American Institute of Physics.* [S0034-6748(97)03405-9]

I. INTRODUCTION

The loop-gap (LG) resonator is a simple but powerful microwave resonance circuit consisting of a conducting loop (the inductance) and a gap (the capacitance). Early experiments using LG resonators were reported by Decorps and Fric,[1] operating at 210 MHz, and by Hardy and Whitehead,[2] who extended the upper frequency to 2 GHz. For electron paramagnetic resonance (EPR) experiments Froncisz and Hyde[3,4] advanced the LG resonator to 10 GHz and later even to Q-band frequencies.[5] The loop-gap resonator has also been used in NMR[6] and several optically detected magnetic resonance (ODMR) investigations.[7,8] In these experiments the resonance frequency was shifted by introducing a dielectric material (mica plate, sapphire) into the gap. Unfortunately, this leads to an inhomogeneous microwave field distribution inside the resonator. Schmidt and collaborators[9] used a so-called reentrant cavity operating at S-band frequencies.

We used a different configuration based on the bridged loop-gap (BLG) resonator concept originally invented by Forrer and collaborators[10,11] for pulsed X-band EPR and electron-nuclear double resonance (ENDOR) spectroscopy. In this design the capacitance of the resonator is not defined by the volume between the two open ends of the loop but by the volume between the loop ends and the bridges (Fig. 1). This leads to a more homogeneous microwave magnetic field distribution over the sample volume and confines the electric field to regions outside the sample volume.[11] For our pulsed zero-field ODMR, frequency tuning of the resonator is necessary to achieve resonance with the zero-field splittings of the photoexcited triplet molecules. The BLG concept is well adapted to the problem because of the following reasons: on the one hand the resonator dimensions remain reasonably small even at S- and L-band frequencies, on the other hand

the resonator is tunable over a wide frequency range by changing the distance between bridges and loop.

II. DESCRIPTION OF THE RESONATOR

A. Construction

Our probehead/resonator construction had to fulfill the following requirements:

(1) light access in two perpendicular axes for ODMR experiments,
(2) frequency tuning at liquid helium temperatures.

The BLG structure is mounted onto a quartz tube that is fixed in a resonator holder containing the tuning mechanism (see Fig. 2). The tuneable BLG concept will now be explained in further detail.

A typical one loop-two gaps structure is shown in Fig. 1. Two nearly half cylindrical metal layers are fixed on a quartz tube ($d_{\mathrm{in}}/d_{\mathrm{out}}=4$ mm/6 mm or 6 mm/8 mm, length: 10 cm) without having electrical contact. They form the basic loop-gap resonator. The metal layers are fixed either by gluing thin copper foils (thickness: 2–10 μm, length: 20 mm) onto the quartz tube or by painting a gold suspension directly onto the quartz tube (<2 μm).[11] As will be shown, the most important parameter fixing the range of accessible resonance frequencies is given by the diameter of the quartz tube. To ensure optical access, one of the metal layers contains a hole ($d=3$ mm). In our experiments, this enables the detection of the phosphorescence of the sample, while the excitation is done parallel to the quartz tube z axis (Fig. 1).

The magnetic field distribution of the resonator has its maximum inside the quartz tube, the electric field is located mainly between the gaps and the bridges. Therefore mechanical adjustment of the bridge/gap distance changes the
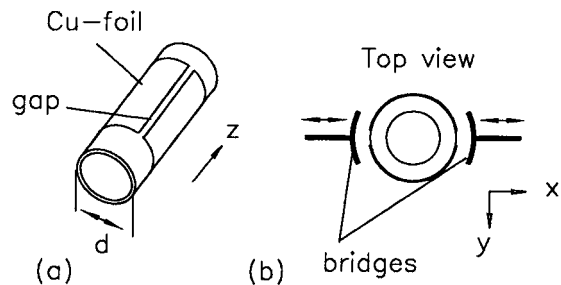
FIG. 1. The bridged loop-gap (BLG) resonator showing the principal components. (a) Copper foils (thickness: 10 μm) fixed on a quartz tube forming the basic loop-gap structure. (b) Top view of basic loop-gap structure in its ''bridged'' configuration with both bridges moveable along the x axis (see the text).

capacitance of the resonance circuit and allows a frequency tuning to the magnetic resonance condition.

In our design the resonator is tuned by simultaneous antiparallel shift of two bridges in a direction normal to the gaps, as is shown in Fig. 1. The curvature of the bridges (length: 20 mm) is adjusted to the outer diameter of the quartz tube to minimize stray fields and ensure an effective variation of the capacitance. As the resonance frequency is very sensitive to a change in distance between bridge and gap (≤ 2 GHz/mm depending on the absolute position of the bridges), a reduction gear had to be designed to ensure fine tuning capability of the resonator frequency with high stability of the bridge/gap distance (Fig. 2) even at low temperatures.

To suppress microwave radiation of the resonator and an unwanted decrease of the quality factor, the whole resonator is surrounded by a metallic shield ($d_{in} = 30$ mm, $d_{out} = 32$ mm), containing two optical windows of 10 mm diameter. The shield diameter has also an effect on the resonance frequency of the resonator. An increase in diameter of the microwave shield while keeping the rest of the resonator geometry constant reduces the resonance frequency.[11] In our design the shield cylinder had to be large enough to allow the bridges to be shifted away from the gap by up to 6 mm.

All metallic parts of the BLG resonator holder of Fig. 2 are made out of brass.

B. Coupling and tuning

A loop-gap resonator can be coupled to external microwave circuits by both inductive and capacitive means.[2,3] We chose an inductive loop that utilizes the microwave magnetic fields at either end of the resonator. The degree of coupling is adjusted by changing the distance of the coupling loop relative to the resonator. The loop itself is part of a semirigid microwave coaxial line, one of the ends forming a loop (Fig. 2). The coupling loop just fits onto the outer diameter of the quartz tube to reduce mechanical instabilities, but with enough spacing to guarantee smooth variation of the coupling parameter. For pulsed EPR and ODMR experiments this coupling mechanism is stable enough even at low temperature. The frequency range of the BLG for the fine-tuning procedure can be set to different microwave frequency bands
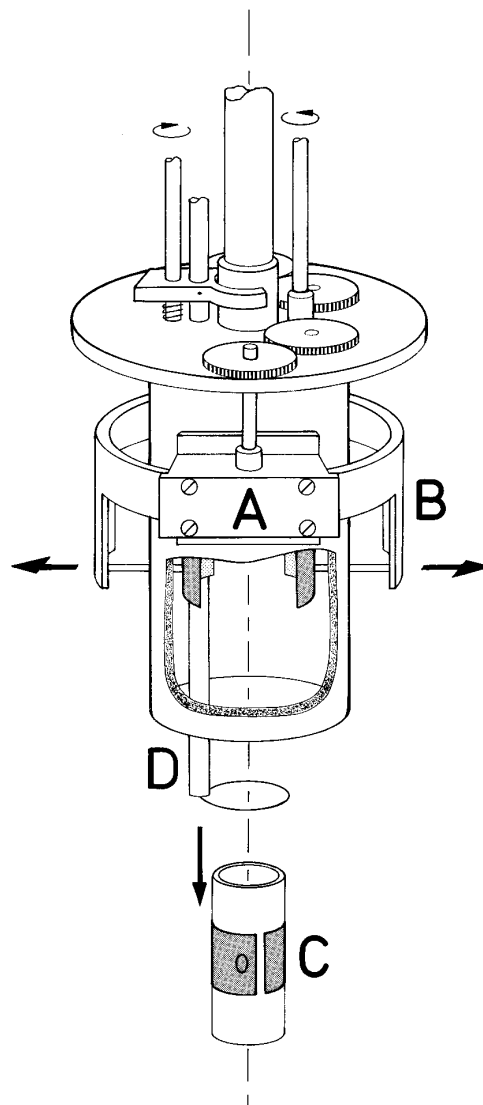

FIG. 2. Probehead with BLG resonator and coupling loop. A: reduction gear for bridge drive, B: bridge holder, C: BLG resonator, D: microwave semi-rigid cable with coupling loop.

by exchanging the inner quartz tube containing the loop-gap structure. Both the reduction of the diameter of the quartz tube and the reduction of the number of gaps increases the resonance frequency. Although for the LG resonator a semi-empirical equation has been established to calculate the resonance frequencies from the geometrical and electrical parameters,[3] for the BLG resonator a similar expression was not yet given.

For the BLG working at C-band frequencies we designed a structure (one loop - two gaps) of an outer diameter of 6 mm. The gaps can be considered as a serial circuit of capacitors and, therefore, one can reduce the entire capacitance of the resonance circuit by increasing their number. An upper frequency of 8.2 GHz was obtained by driving the bridges far away from the gaps, and the lowest frequency was 3.9 GHz. Figure 3 shows the dependence of the resonance frequency on the bridge/gap distance at room temperature, as measured with the resonator of $d_{out} = 6$ mm. This
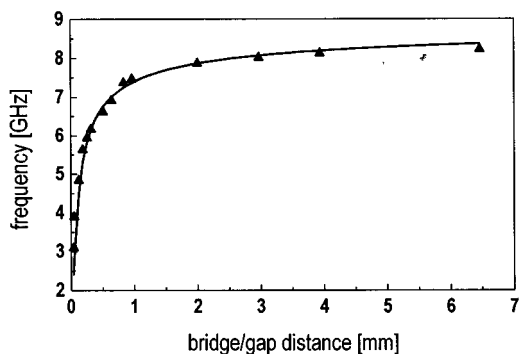
FIG. 3. Resonance frequency dependence on the distance between gap and bridges for the BLG resonator with $d_{outer} = 6$ mm, (▲) measured frequencies, (−) simulation using equation (1) with the parameters $\nu_{max} = 8.8$ GHz, $\nu_{min} = 2.6$ GHz, $d_0 = 0.037$ mm.
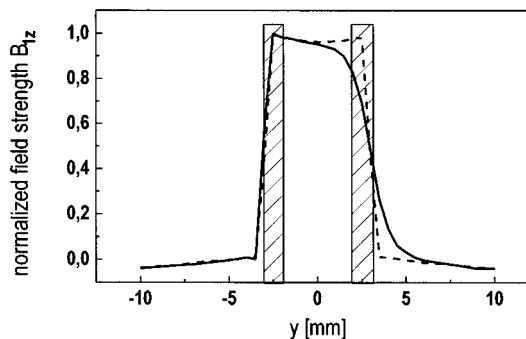

FIG. 4. B_1 field distribution of the BLG resonator along the y axis ($x=0$, $z=0$) calculated with MAFIA. The z component of the microwave B_1 field is reduced by 15% on the side of the optical window (solid line) compared to a resonator without optical window (dashed line). The shaded areas represent the quartz tube walls.

frequency dependence of the BLG resonator can be described by

$$\nu(d) = \frac{1}{\sqrt{\nu_{max}^{-2} + \dfrac{\nu_{min}^{-2} - \nu_{max}^{-2}}{1 + \dfrac{d}{d_0}}}}, \qquad (1)$$

where d is the bridge/gap distance, ν_{max} and ν_{min} are the frequencies for maximum and minimum bridge/gap distance and d_0 is the minimum bridge/gap distance. The measurements of Fig. 3 are well described with $\nu_{max} = 8.8$ GHz, $\nu_{min} = 2.6$ GHz and $d_0 = 0.037$ mm.

The S-band frequency range could be realized with a BLG structure of 8 mm outer diameter and only one gap. With this design frequencies between 1.9 and 3 GHz were accessible (Table I).

It turned out that once the resonator is coupled, fine tuning of the frequency can be done without severely changing the degree of coupling. The loaded Q values of the resonators at liquid helium temperature are listed in Table I. As the resonator was planned to be used in coherent pulsed microwave experiments, a good homogeneity of the induced magnetic field is required at the sample position. The field distribution of the resonator fundamental mode was calculated by using the MAFIA program (MAFIA is a software package to determine three-dimensional electromagnetic field distributions[12]). The results show that the magnetic flux lines are concentrated inside the tube and the quartz tube walls along the z axis of the resonator. In proximity to the optical

window, the magnetic flux lines are distorted towards the outside of the tube. As a consequence the magnetic field strength in z direction, B_{1z}, is reduced, as is shown in Fig. 4, where resonators with and without optical window ($d=3$ mm) are compared. The plot shows a trace of the z component of the microwave B_1 field in the x-y plane of the resonator at the sample position ($z=0$, $x=0$). Without optical window the B_1 distribution is symmetric relative to $y=0$ (dashed line). The optical window at $y=+3$ mm breaks the symmetry of the distribution and reduces the magnetic field strength inside the resonator by up to 15% of the center field strength (solid line). If the sample is confined to $y=\pm 1$ mm, as is the case for our sample holder, the reduction of B_1 can be limited to 5% over the sample volume.

Figure 5 shows the excellent field homogeneity of the BLG resonator along the z axis in the center of the quartz tube ($x=0$, $y=0$). Only near the window region ($z=\pm 1.5$ mm) the magnetic field is reduced by $\approx 3\%$ (solid line).

Dielectric losses due to electric field components interacting with the sample remain very small within the resonator since the electric field is located mainly at the outside of the quartz tube.[11] Besides the resonance mode described above, the BLG resonator has also an unwanted resonance mode without strong magnetic field at the sample position.
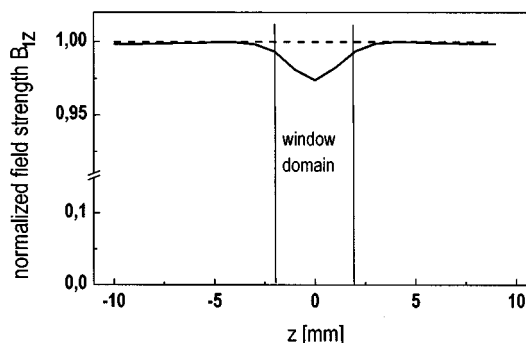
TABLE I. Characteristic parameters of the tuneable bridged loop-gap resonators.

Outer diameter (mm)	Specification	Frequency range (GHz)	Q value (loaded)
6	1 loop/1 gap	>3	
6	1 loop/2 gaps	3.9-8	350-450
8	1 loop/1 gap	1.9-3	600-750
8	1 loop/2 gaps	>2.9	

FIG. 5. B_1 field distribution of the BLG resonator along the z axis ($x=0$, $y=0$) calculated with MAFIA. The B_{1z} component is reduced by $\approx 3\%$ in the window area (solid line) in comparison to the resonator without optical window (dashed line).
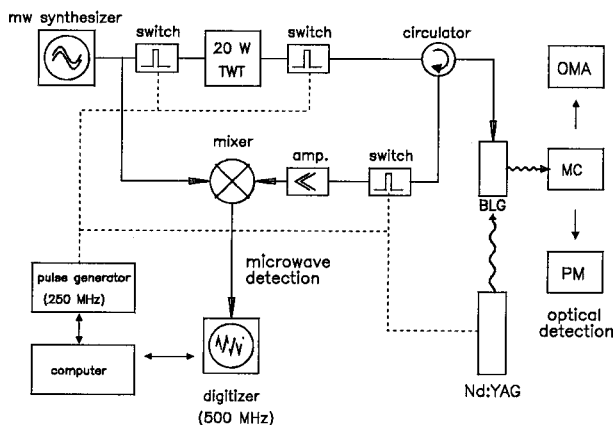
FIG. 6. Experimental setup for pulsed microwave ODMR experiments in zero magnetic field including the option for microwave detection. TWT: traveling wave tube amplifier; MC: monochromator; PM: photomultiplier; OMA: optical multichannel analyzer; amp.: GaAs low noise amplifier; Nd:YAG: pulsed laser.

The proper mode for ODMR experiments can be identified by tuning the resonator. While the resonance of this mode is shifting to higher frequencies by increasing the distance between bridge and gap, the "wrong" mode shifts to lower frequencies. Apparently the wrong mode is located between the bridges and the outer shield of the resonator holder and is present for both loop-gap configurations used. Its behavior is the same for room and liquid helium temperatures.

III. EXPERIMENTAL SETUP FOR ODMR

The experimental setup for zero-field pulsed microwave ODMR experiments, including the option for microwave detection, is shown in Fig. 6. All experiments were performed at pumped helium temperature (1.4 K) in a bath cryostat. The molecular crystal samples (2000 ppm acridine in fluorene, 1000 ppm benzophenone in a 4,4′-dibromodiphenylether matrix) were excited with the third harmonic ($\lambda = 355$ nm, pulse length 12 ns) of a pulsed Nd:yttrium aluminum garnet (YAG) laser. The phosphorescence light was analyzed by a monochromator in combination with either a photomultiplier or an optical multichannel analyzer (OMA). The OMA was operated in a gated mode so that the diode array was sensitive only during the gate time ($t_{gate} = 10$ ms).

In addition to the optical detection a microwave detection of the magnetic resonance is possible using a mixer configuration with a circulator, since the BLG resonator is operating in reflection (Fig. 6). The microwave pulses are formed on the low microwave power level of the synthesizer (+10 dBm) with subsequent amplification by a 20 W traveling-wave tube (TWT). The master clock of the experiment, which is used to trigger the laser as well as the OMA and all the mw switches, is a pulse generator with a time resolution of 4 ns.

IV. EXPERIMENTS

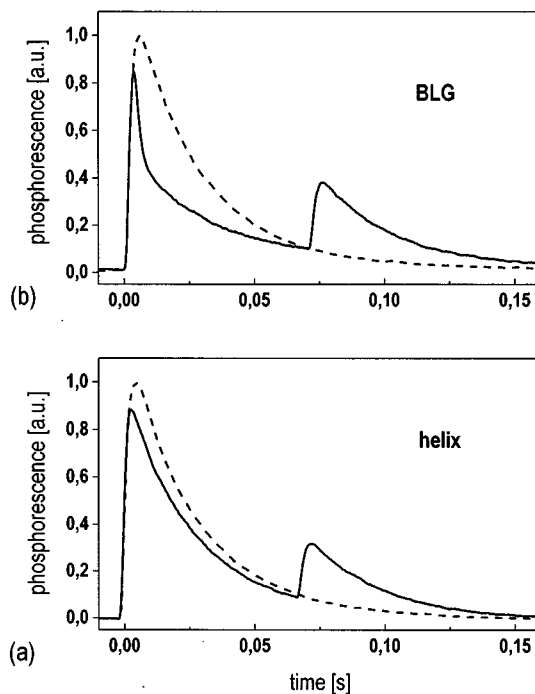In this section we compare pulsed experiments with the BLG to those with the broadband slow-wave helix structure.

FIG. 7. MIDP experiments on the photoexcited triplet state of acridine: comparison between slow-wave helix (a) and BLG resonator (b). The MIDP time profiles are compared to the phosphorescence without microwave irradiation (dashed lines). The ODMR transition was excited at the center frequency of 2.473 GHz ($|T_x\rangle - |T_z\rangle$ transition). The phosphorescence was monitored using the photomultiplier with a low-pass time filter.

The first type of experiment is microwave induced delayed phosphorescence (MIDP).[13] Two strong microwave pulses of identical duration are applied with a certain delay after the photoexcitation of the molecule, while the time behavior of the phosphorescence is monitored. Due to a spin selective inter system crossing (ISC), the triplet $|T_x\rangle$ level of acridine contains more than 90% of the entire triplet population[14] if the S_0-S_1 transition of the acridine guest molecules is selected for excitation. At 355 nm excitation wavelength, however, the guest molecule triplet state is populated via the excited host molecule triplet state. This process causes a reduction of the above mentioned ISC selectivity and results in a less effective population of the $|T_x\rangle$ level. If a microwave π pulse is applied to the $|T_x\rangle - |T_z\rangle$ transition, the population is transferred to the $|T_z\rangle$ level having a phosphorescence rate of $k_z \approx 4$ s^{-1} ($k_x \approx 89$ s^{-1}).[14] As a consequence, the first microwave π pulse reduces the phosphorescence intensity while the second π pulse increases the phosphorescence intensity by repopulating the strongly radiating triplet level $|T_x\rangle$.

Figure 7 shows the MIDP experiment on acridine using the BLG resonator and the slow-wave helix, respectively. The first mw pulse is set 2 ms after the laser excitation, the second one after a delay of 75 ms. The MIDP effect reaches its maximum when the pulses are π pulses ($t^{\pi}_{BLG} = 40$ ns, $t^{\pi}_{helix} = 300$ ns). It is clearly seen that the change in phosphorescence is considerably enhanced using the BLG. This is due to the stronger B_1 field in the BLG resonator ($B_1 \approx 4.5$ G) compared to the B_1 field in the helix ($B_1 \approx 0.6$ G). As the
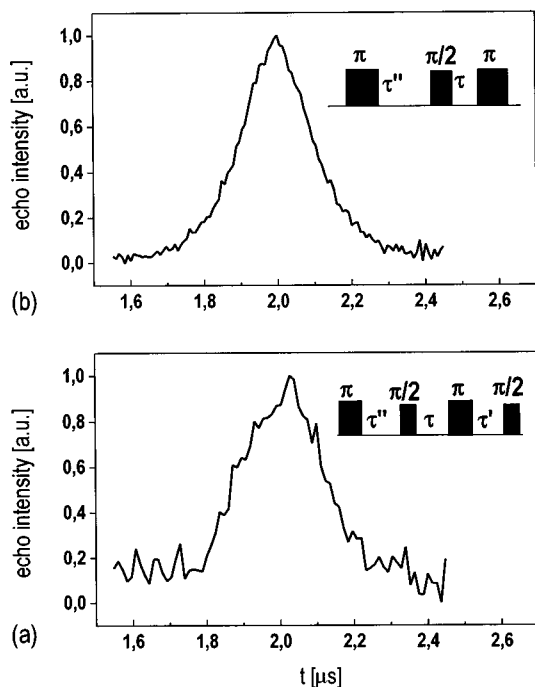
FIG. 8. Optically (a) and microwave detected (b) two-pulse echo experiment on the triplet state of acridine (2.473 GHz) using the microwave BLG resonator ($\tau'' = 75$ ms, $\tau = 2$ μs).
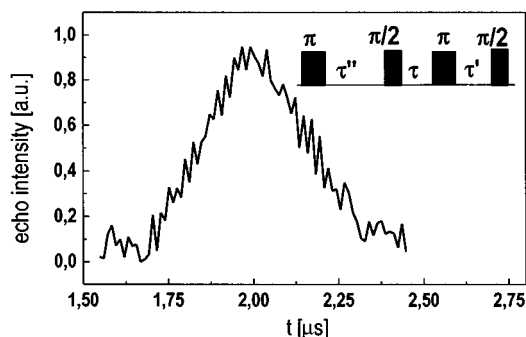

FIG. 9. Optically detected two-pulse echo experiment on the triplet state of acridine (2.473 GHz) using the slow-wave helix. The echo was recorded under identical conditions as those with the BLG resonator ($\tau'' = 75$ ms, $\tau = 2$ μs).

linewidth of the investigated ODMR transition is about 5 MHz, the helix is not able to excite the whole line, therefore the microwave effect is smaller.

The second type of experiment we present is a zero-field Hahn echo[15,16] using the following pulse sequence:

$$\underbrace{\pi - \tau''}_{\text{preparation}} - \underbrace{\pi/2 - \tau - \pi - \tau'}_{\text{evolution}} - \underbrace{\pi/2}_{\text{detection}} \, .$$

(2)

During the preparation sequence the π pulse transfers the population to the slowly decaying $|T_z\rangle$ level. After the time τ'' (≈ 80 ms) the population of the $|T_x\rangle$ level has decayed to 10^{-4} of its initial value due to its faster phosphorescence rate, while the $|T_z\rangle$ population has only decayed to 75% of its initial value. The evolution period consists of a two-pulse echo sequence forming an echo signal at the time $\tau' = \tau$ after the inversion pulse. The detection is done by an additional $\pi/2$ probe pulse which is necessary to transform the coherent echo signal into an optically detectable population difference.[17] In the case of microwave detection of magnetic resonance the echo signal is measured, of course, without this $\pi/2$ probe pulse.

The zero-field echoes of triplet state acridine are shown in Figs. 8 and 9. For the optical detection the OMA was gated for 10 ms after the $\pi/2$ probe pulse to accumulate the phosphorescence changes due to the Hahn-echo pulse sequence. The experiment was repeated several times for a fixed time τ'. With this technique the echo is recorded point by point in the time domain by stepping the time τ'. The use of the tunable BLG resonator also allows a microwave de-

tection in zero field (Fig. 6). While microwave detection of the Hahn echo is feasible only with the microwave resonator, optical detection is possible both for the BLG and the helix (Figs. 8 and 9). Using the helix the Hahn-echo is approximately a factor of 2 broader than when using the BLG resonator. This is related to the different B_1 fields for helix and resonator when applying the same microwave power. As the helix cannot excite the entire zero-field transition, the echo width in the time domain is broadened compared to the resonator.

The choice between microwave and optical detection of magnetic resonance depends on the properties of the sample under study. Since it is always possible to transform a population difference (longitudinal magnetization) into a transverse magnetization and vice versa, both methods can principally be applied. A comparison of the sensitivity of both methods has been done by Schmidt and collaborators.[9] They showed that optical detection is only much more sensitive if the echo signal can be converted into a pulse of light against zero background. In practice, however, noise arising from background radiation is usually present so that often it might be more advantageous to use microwave detection.

Finally we present a two-pulse echo experiment in the C band. The measurements on the $|T_x\rangle - |T_z\rangle$ transition of the excited benzophenone molecule ($\nu = 5.226$ GHz) are performed using the tunable one loop/two gaps resonator with an outer diameter of 6 mm. Figure 10 shows the microwave-detected echo experiment with a π-pulse length of $t^{\pi}_{\text{BLG}} = 48$ ns ($t^{\pi}_{\text{helix}} = 260$ ns).

In summary we have described a tuneable microwave bridged loop-gap resonator for the S and C bands allowing both optical and microwave detection of magnetic resonance transitions. The resonator concept allows a change of the accessible frequency range simply by exchanging the quartz tube containing the loop-gap structure. Due to the BLG design a high microwave field homogeneity is achieved over the sample volume while dielectric losses are strongly reduced. This is because the electric field is confined to regions outside the sample volume. The microwave pulse lengths—compared to the conventional slow-wave helix—could be reduced nearly by an order of magnitude allowing a more
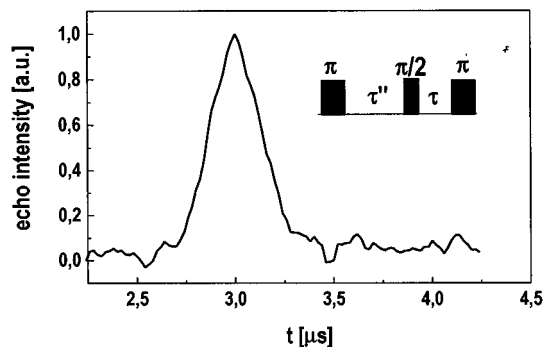
FIG. 10. Microwave detected two-pulse echo experiment on the triplet state of benzophenone (5.226 GHz) using the BLG resonator ($\tau'' = 10$ ms, $\tau = 3$ μs).

effective excitation of ''broad'' zero-field transitions and a better time resolution for pulsed experiments.

ACKNOWLEDGMENTS

[1] M. Decorps and C. Fric, J. Phys. E **5**, 337 (1972).
[2] W. N. Hardy and L. A. Whitehead, Rev. Sci. Instrum. **52**, 213 (1981).
[3] W. Froncisz and J. S. Hyde, J. Magn. Reson. **47**, 515 (1982).
[4] J. S. Hyde and W. Froncisz, in *Advanced EPR*, edited by A. J. Hoff (Elsevier, Amsterdam, 1989), Chap. 7.
[5] W. Froncisz, T. Oles, and J. S. Hyde, Rev. Sci. Instrum. **57**, 6 (1986).
[6] M. F. Koskinen and K. R. Metz, J. Magn. Reson. **98**, 576 (1992).
[7] A. J. Hoff, Chap. 18 in Ref. 4.
[8] T. Kirski, B. Stein, F. Rothamel, and C. von Borczyskowski, Appl. Magn. Reson. **2**, 217 (1991).
[9] J. Schmidt and J. H. van der Waals, in *Time Domain Electron Spin Resonance*, edited by L. Kevan and R. N. Schwartz (Wiley, New York, 1979), Chap. 9.
[10] J. Forrer, S. Pfenninger, J. Eisenegger, and A. Schweiger, Rev. Sci. Instrum. **61**, 11 (1990).
[11] S. Pfenninger, J. Forrer, and A. Schweiger, Rev. Sci. Instrum. **59**, 752 (1988).
[12] Professor Dr. Ing. T. Weiland, Institut für Hochfrequenztechnik, TH Darmstadt.
[13] K. P. Dinse and C. J. Winscom, J. Chem. Phys. **68**, 1337 (1978).
[14] M. Kinoshita, N. Iwasaki, and N. Nishi, Appl. Spectrosc. Rev. **17**, 95 (1981).
[15] E. Hahn, Phys. Rev. **80**, 580 (1950).
[16] W. G. Breiland, C. B. Harris, and A. Pines, Phys. Rev. Lett. **30**, 158 (1973).
[17] R. P. Feynman, F. L. Vernon, and R. W. Hellwarth, J. Appl. Phys. **28**, 49 (1957).